DOI:10.5937/jaes0-35499
Paper number: 20(2022)3, 974, 673-687
*www.engineeringscience.rs * ISSN 1451-4117 * Vol.20, No 3, 2022*

INVESTIGATION OF CONVENTIONAL AND ASPHALTIC UNDERLAYMENT TRACK BEHAVIORS SUBJECTED TO FREIGHT TRAIN LOAD: MECHANISTIC APPROACH

Dian M. Setiawan

Department of Civil Engineering, Jl. Brawijaya,Bantul,Yogyakarta, Indonesia
**diansetiawanm@ft.umy.ac.id*

The load characteristics in terms of the carrying capacity and the train operation speed limit Indonesia's conventional track capability. In this study, the behaviors of Indonesia's conventional tracks and the proposed asphaltic underlayment tracks under cyclic loading conditions of the low-speed Babaranjang (long-chain coal) freight trains have been evaluated using the finite element package Abaqus/CAE considering linear elastic behavior of materials. The numerical modeling was applied on three different layer thicknesses of sub-ballast in Indonesia's conventional tracks and three different layer thicknesses of asphalt in asphaltic underlayment tracks to investigate the vertical compressive stress, horizontal-vertical-maximum strain, and deformation behaviors. According to the numerical simulation, the measurements indicate that the asphaltic underlayment tracks are superior to Indonesia's conventional tracks. Furthermore, a 15 cm of asphalt layer in the asphaltic underlayment tracks demonstrates promising performance in the future of Indonesia's railway systems. The asphaltic underlayment tracks are expected to serve the heavier and higher speed Babaranjang freight trains with longer service life and lower life cycle cost than Indonesia's conventional tracks.

Keywords: asphaltic underlayment track, conventional track, freight trains, mechanistic, deformation, vertical compressive stress

1 INTRODUCTION

The Indonesian government has adopted the MP3EI master plan, a strategic economic corridor approach, to expand and accelerate Indonesian economic development. One of the approaches promoted and adopted by Indonesia's Ministry of Transportation is the rail modal shift to achieve green logistics, in other words, to reduce greenhouse gas emissions in the long term. Along with the many activities involving the realization of economic development through the strategic corridors, priority projects at the top level promote the rail modal shift. Within the MP3EI, several strategies aim to expand freight rail transportation systems. On Sumatra railway lines, the aim is to increase rail capacity to support palm oil, coal, and steel industries. Rail construction is also planned on Kalimantan Island to transport coal [1;2]. To achieve it, in 2011-2015, Indonesia's government had improved the role of trains to handle long-distance cargo transport on Sumatra and Java Islands. In 2016-2020, Trans Sumatra Railway was developed to connect production centers and transport nodes. By 2021-2025, it is expected that rail transport will carry out effective operations as the main alternative to road freight [2;3]. It is anticipated that the transport of freight by rail will increase network capacity, in addition to reducing the negative impacts caused by the dominance of road freight, including congestion and infrastructure damage. It has potential benefits for infrastructure managers, suppliers, and passengers.

Of the 8,357 km of total Indonesia's railway network in 2017, only 5,107 km are operated [4], and most are traditional ballasted tracks. Unfortunately, the Indonesian railway network remains of a low standard, with the maximum axle load of 18 tons, the relatively light rail weight of 54 kg/m (R54) (see Table 1), and the low freight train operating speed between 45 km/h to 70 km/h. Therefore, the load characteristics, rail strength, carrying capacity, and the train operation speed limit the capability of Indonesia's railway network.

Table 1.Indonesia's conventional tracks for narrow gauge 1,067 mm [5]

Rail track class	**Passing tonnage (tons/year)**	**Design speed (km/hour)**	**Axle load (tons)**	**Rail type**	**Sleeper type** / **Distance between sleeper (mm)**	**Ballast thickness (cm)**
I	> 20.10^6	120	18	R.60/R.54	Concrete / 600	30
II	10.10^6 - 20.10^6	110		R.54/R.50	Concrete/Wooden / 600	30

Rail track class	Passing tonnage (tons/year)	Design speed (km/hour)	Axle load (tons)	Rail type	Sleeper type / Distance between sleeper (mm)	Ballast thickness (cm)
III	5.10^6 - 10.10^6	100		R.54/R.50/R.42	Concrete/Wooden / 600	30
IV	$2.5.10^6$ - 5.10^6	90		R.54/R.50/R.42	Concrete/Wooden / 600	25
V	< $2.5.10^6$	80		R.42	Wooden/Steel / 600	25

Indonesia's current rail freight market is small due to the total freight load limited by low permitted train operating speed and axle load capacity. According to Dikun [6], despite a better-integrated system on Java Island, the rail freight figure is lower. The train operation on Java Island is dominated by the high passenger capacity with 95% of the national level, and 90 billion tons of goods lifted in 2008 were delivered by rail freight on Sumatra and Java Islands. Eighty percent of goods lifted are on Sumatra Island, with over 15 billion tons of goods. In addition, there has been an increase in rail freight use in Sumatra since 2007 due to coal transported by Babaranjang (Long Chain Coal) trains (Fig. 1), fertilizers, palm oil, cement, and container traffic [2].

Fig. 1. Babaranjang (long chain coal) train in South Sumatera, Indonesia

The conventional ballasted track-bed is still an important option for Indonesia's railway substructures due to its low cost and easy construction. However, most freight train derailments on Sumatra rail lines are caused by conventional track deterioration, weak performance, and poor construction and maintenance work. The latest freight train accidents occurred near MuaraEnim Regency, South Sumatera Province, on December 11, 2021 [7] and March 17, 2018 [8]. Therefore, there is an urgent need to develop and consider alternative rail track types that can provide stronger and better structures in minimizing permanent structural deformation and, at the same time, increasing the safety of train operation.

In Indonesia, maintenance of traditional ballasted tracks is both costly and difficult to be managed effectively. Hence, Track Quality Index (TQI) has been adopted to quantify and monitor conventional track degradation. Based on the results of track line geometry measurement by the track recording car, a geometry tolerant value is given to decide the follow-up of measurement, whether it needs to perform immediate maintenance, train speed restriction-reduction, or track rehabilitation [9]. However, most of the TQI calculations have suggested Indonesia's railway maintenance stakeholder increase the thickness of the ballast layer in several black spots where the train derailments have occurred, from 30 cm as a regular value to 50 cm, to mitigate structural deformation and rail irregularities. Unfortunately, no further research investigated Indonesia's conventional track performance with a ballast layer almost two times thicker than the regular thickness.

Several works have been performed with the aims to enhance the conventional ballasted track-bed performance to prevent structural deterioration due to the passing of trains with higher speed and heavier axle load [10-24]. In addition, various studies have been conducted to develop unconventional rail track-bed designs and evaluate their performance to meet the requirements of high-speed railway systems in terms of track vibration, noise, and service life [25-41].

However, there are still a limited number of studies aiming to investigate the behavior of conventional and unconventional tracks subjected to heavy and low-speed freight trains. Unconventional tracks mainly refer to concrete or asphalt that replaces ballast material, which can be found largely in civil structures for high-speed and light rail lines. The main reason for the limited use of concrete on the slab track is due to the high construction costs associated with its foundation preparations, which are 2.5 times higher than conventional tracks [42]. Asphaltic underlayment tracks were selected as one of the rail track types studied. Based on several studies and

field experiences, the asphalt layer laid below the ballast layer could dampen the vibration and reduce the stress level on the subgrade, leading to a reduction in the maintenance needs [32; 43-46].

This paper focuses on the full-mechanistic approach in analyzing the performance of Indonesia's conventional tracks subjected to the heavy and low-speed Babaranjang freight trains and compares the results with the response of the asphaltic underlayment tracks. A method of modeling the conventional and asphaltic underlayment tracks is presented here using the commercial finite element software Abaqus to investigate the effect of various sub-ballast and asphalt layer thicknesses on the mechanical characteristics of Indonesia's conventional tracks and the proposed-new rail track-type design, asphaltic underlayment tracks, in terms of vertical compressive stress, horizontal-vertical strain, and deformation

2 RESEARCH METHOD

2.1 Geometric and dimension of rail tracks

As presented in Table 2, the thickness in Case 1A represents the thin sub-ballast layer in the conventional tracks, Case 1B depicts the normal sub-ballast layer in the conventional tracks (classified as the 1st Class in Indonesia's railway systems), and Case 1C portrays the thick sub-ballast layer in the conventional tracks.

Table 2.Geometric and dimension of the conventional tracks

Conventional track layer	**Case 1A**	**Case 1B**	**Case 1C**
Ballast	30 cm	30 cm	30 cm
Sub-Ballast	30 cm	40 cm	50 cm
Subgrade	330 cm	330 cm	330 cm
Total	390 cm	400 cm	410 cm

As displayed in Table 3, the asphalt layer thickness in Case 2A, Case 2B, and Case 2C illustrates the thin, medium, and thick asphalt layers in the asphaltic underlayment track systems.

Table 3.Geometric and dimension of the asphaltic underlayment tracks

Asphaltic underlayment track layer	**Case 2A**	**Case 2B**	**Case 2C**
Ballast	30 cm	30 cm	30 cm
Asphalt Layer	15 cm	20 cm	25 cm
Subgrade	330 cm	330 cm	330 cm
Total	375 cm	380 cm	385 cm

The measurement positions of vertical compressive stress at the top of the subgrade and displacement at the sleeper's surface and the subgrade layer are demonstrated in Fig. 2 for the conventional tracks and Fig. 3 for the asphaltic underlayment tracks, respectively.

2.2 Material properties

All materials in the conventional and asphaltic underlayment tracks evaluated in this study are considered linear elastic behavior. The material parameters comprise the elastic modulus, Poisson's ratio, and mass density. Material inputs for the conventional and asphaltic underlayment track simulation are exhibited in Table 4 and Table 5, respectively.

Table 4. Material inputs for modeling of the conventional tracks

Conventional track layer	**Elastic modulus E (MPa)**	**Mass density ρ (kg/m^3)**	**Poisson's ratio v**
Sleeper [47]	29,100	2,300	0.30
Ballast [48]	130	1,900	0.20
Sub-Ballast [48]	120	1,900	0.30
Subgrade [47]	80	2,000	0.30

Table 5. Material inputs for modeling of the asphaltic underlayment tracks

Asphaltic Underlayment Track Layer	Elastic Modulus E (MPa)	Mass Density ρ (kg/m^3)	Poisson's Ratio v
Sleeper [47]	29,100	2,300	0.30
Ballast [48]	130	1,900	0.20
Asphalt Layer [48]	4000	2,400	0.35
Subgrade [47]	80	2,000	0.30

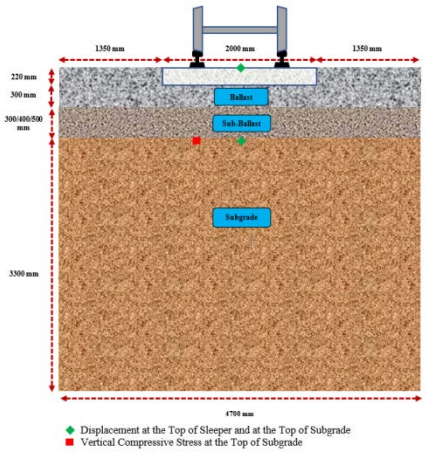

Fig. 2. 2D sketch of the conventional tracks and measurement position

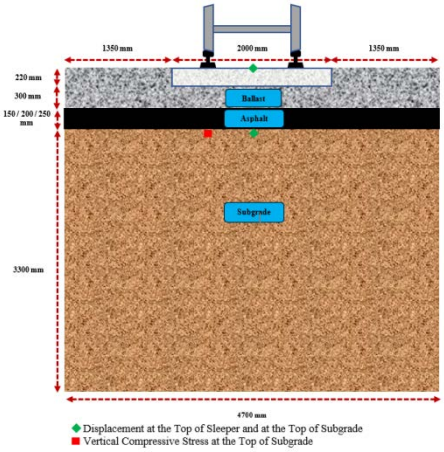

Fig. 3. 2D sketch of the asphaltic underlayment tracks and measurement position

2.3 Cyclic loading

The dynamic wheel load considered in this study was computed according to the Talbot Formula [49] using Eq. 1 and Eq. 2.

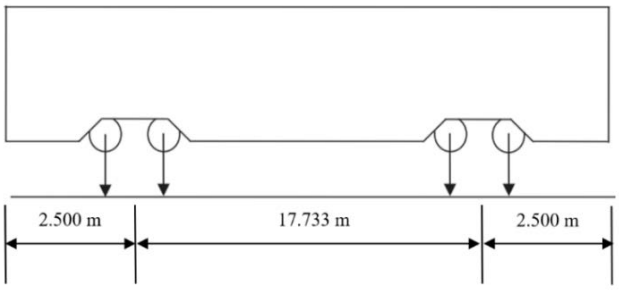

Fig. 4. Distance between two bogies (L_b) [50]

$$I_p = 1 + 0.01\left(\frac{V}{1.609} - 5\right) \quad (1)$$

$$P_d = P_s \times I_p \quad (2)$$

Description:

I_p = Conversion Factor

V = Design Speed, km/hour

P_s = Static Wheel Load of a Train, kg

P_d = Dynamic Wheel Load of a Train, kg

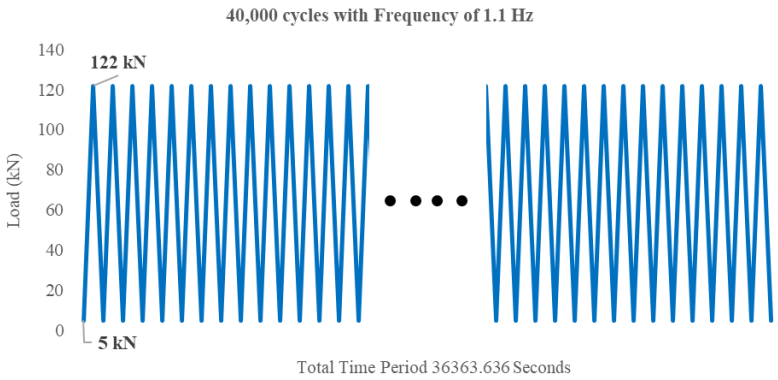

Fig. 5. Cyclic loading configuration

A speed parameter V was applied for 70 km/hr with a static wheel load of 9,000 kg (axle load of 18,000 kg) or 88.3 kN to compute the dynamic wheel load. Then, based on Eq. 1 and Eq. 2, the dynamic wheel load of the Babaranjang freight trains was 12,465 kg or 122 kN. Eq. 3 was utilized to calculate the loading frequency based on the Babaranjang freight train operating speed, 70 km/h, and the distance between the axis of two bogies of the train, 17,733 m (please see Fig. 4).

$$f_b = \frac{V}{L_b} = \frac{70\ {}^{km}/_{h}}{17.733\ m} = \frac{{}^{70{,}000\ m}/_{3600\ s}}{17.733\ m} = 1.1\ \frac{1}{s} = 1.1\ Hz \approx 1\ Hz \qquad (3)$$

In this study, the cyclic loading was implemented with the maximum load of 12,465 kg or 122 kN, frequency 1.1 Hz, and 40,000 cycles, while the total loading time (period) was 40,000 cycles/1.1 Hz = 40,000 seconds, displayed in Fig. 5 and Table 6.

Table 6. Loading time vs. loading amplitude

Period (s)	Load amplitude (N)
0	5000
0.909090909	122000
1.818181818	5000
2.727272727	122000
~	~
~	~
36362.72727	122,000
36363.63636	5,000

2.4 Mechanistic approach

The 2-dimensional modeling of conventional and asphaltic underlayment tracks was performed according to Abaqus/CAE's finite element package. The 2D mesh of the conventional and the asphaltic underlayment tracks is drafted in Fig. 6. A suitable mesh was established for predicting the conventional and asphaltic underlayment track response under cyclic loading. The mesh 50 by 50 mm was used in the ballast, sub-ballast, and subgrade, while the mesh 55 by 50 mm was applied in the sleeper.

Material inputs for the conventional and asphaltic underlayment track simulation are presented in Table 4 and Table 5, respectively. The material properties of the sleeper and subgrade for conventional and asphaltic underlayment tracks were adopted from Lee et al. [47], while the material properties of the ballast, sub-ballast, and asphalt were adopted from Hassan et al. [48]. The material properties of the conventional tracks implemented in this study were the typical value applied in Indonesia's railway systems.

In this numerical simulation, the vertical displacement at the bottom and the horizontal displacement at the side of the model were fixed because the boundary condition was specified as the soil box condition. In addition, the interactions between layers were expected to be fully bonded, and the sleeper was expected to be a rigid material. Therefore, the deformation in the conventional and asphaltic underlayment tracks was determined by subtracting the displacement at the top of the sleeper with the displacement at the top of the subgrade.

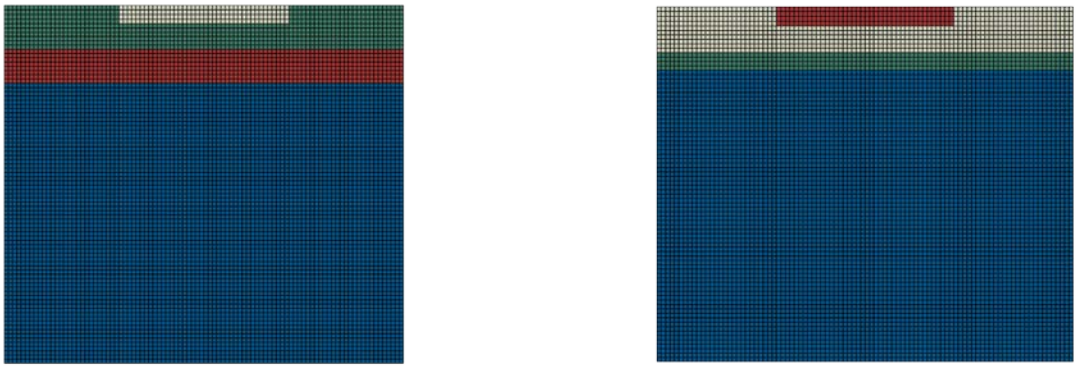

(a) (b)

Fig. 6. 2Dmeshing of the conventional tracks (a) and the asphaltic underlayment tracks (b)

3 RESULTS AND DISCUSSION

3.1 Measurement of vertical compressive stress

Vertical compressive stress was studied by Liu [51], Setiawan [52], and Setiawan [53] to predict the subgrade design life of the ballasted and asphaltic underlayment tracks using a mechanistic-empirical approach. Fig. 7 illustrates the change in vertical compressive stress at the surface of the subgrade layer in conventional and asphaltic underlayment tracks and its magnitude after 40,000 loading cycles. Table 7 demonstrates the regression formula obtained from the numerical simulation results, used to predict the vertical compressive stress at the surface of the subgrade layer in the conventional and the asphaltic underlayment tracks as the loading reached 500,000 times.

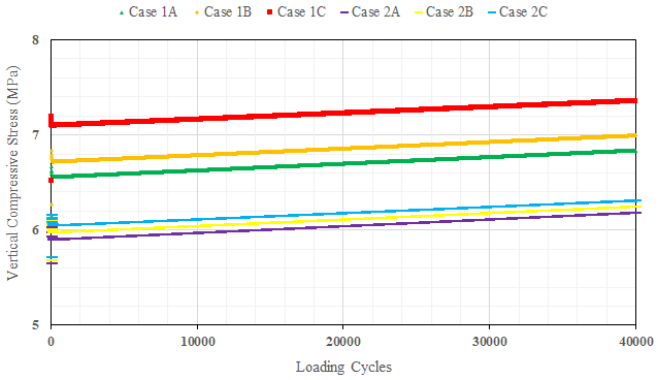

Fig. 7. Change in vertical compressive stress at the surface of the subgrade

Table 7. Vertical compressive stress (MPa) at the surface of the subgrade after 40,000 loading cycles and regression formula to predict vertical compressive stress after 500,000 loading cycles

Track type	Case	Vertical compressive stress (MPa) after 40,000 loading cycles	Regression formula	Predicted vertical compressive stress (MPa) after 500,000 loading cycles
Conventional	1A	6.8381	y = 7E-06x + 6.5484	10.0484
	1B	6.9950	y = 7E-06x + 6.7089	10.2089
	1C	7.3568	y = 7E-06x + 7.0875	10.5875
Asphaltic Underlayment	2A	6.1823	y = 7E-06x + 5.8915	9.3915
	2B	6.2473	y = 7E-06x + 5.9665	9.4665
	2C	6.3097	y = 7E-06x + 6.0380	9.5380

As expected, the thicker ballast and sub-ballast in the conventional tracks, and the thicker ballast and asphalt layer in the asphaltic underlayment tracks, produced higher vertical compressive stress at the surface of the subgrade layer. The investigation results in Table 7 also depict the vertical compressive stress magnitudes of 6.8381 Mpa, 6.9950 Mpa, and 7.3568 MPa for the conventional tracks, consisting of 30 cm (Case 1A), 40 cm (Case 1B), and 50

cm (Case 1C) of sub-ballast, respectively. In other words, the increase of sub-ballast thickness every 10 cm will increase the vertical compressive stress in the conventional tracks between 2% (from 6.8381 MPa in Case 1A to 6.9950 MPa in Case 1B) and 5% (from 6.9950 MPa in Case 1B to 7.3568 MPa in Case 1C).

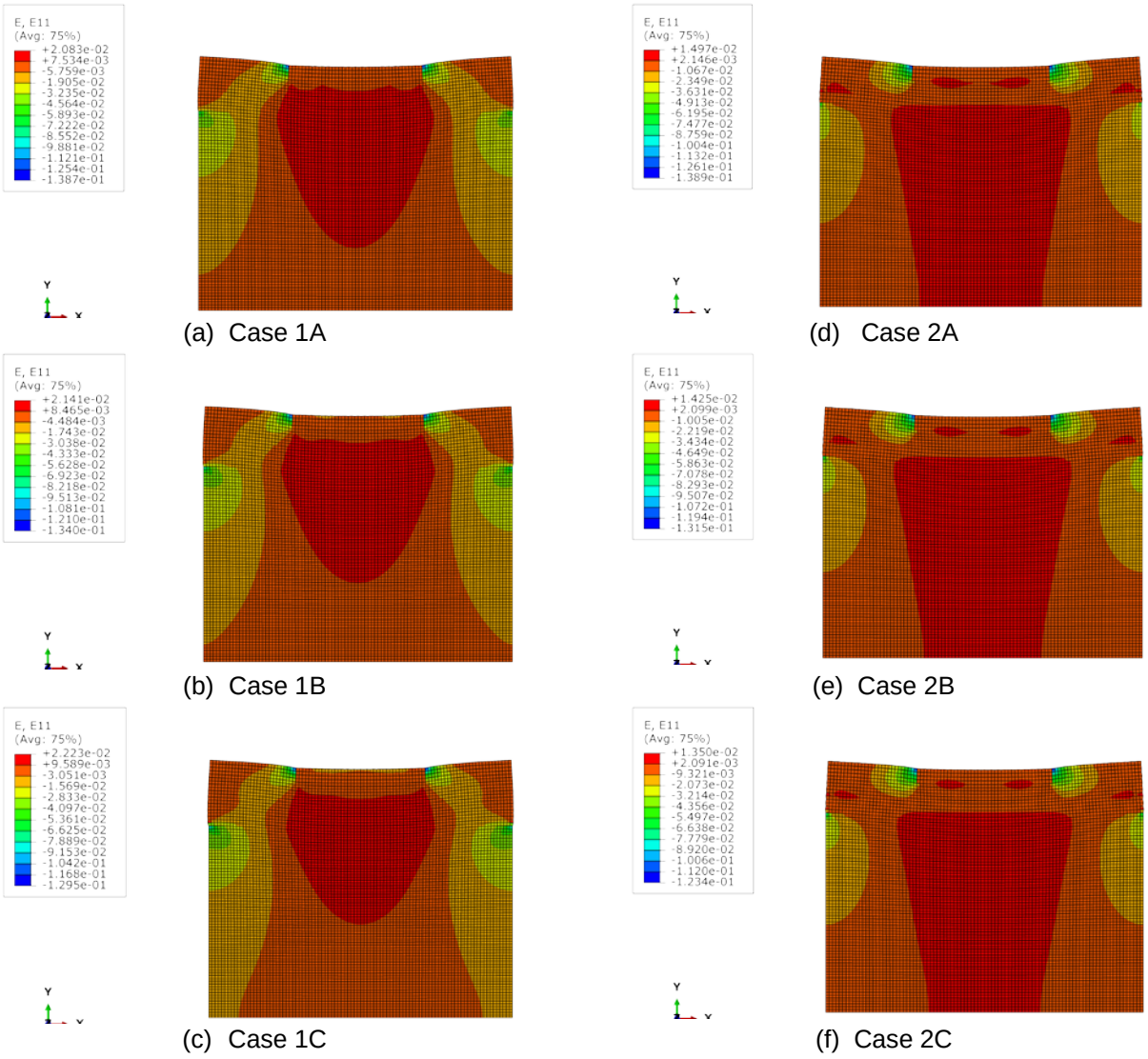

Fig. 8. Horizontal strain distribution in the conventional tracks (a, b, c) and the asphaltic underlayment tracks (d, e, f)

On another side, for the asphaltic underlayment tracks with the asphalt layer thickness of 15 cm, 20 cm, and 25 cm, the measurement outputs acquired vertical compressive stress of 6.1823 MPa (Case 2A), 6.2473 MPa (Case 2B), and 6.3097 MPa (Case 2C), respectively, as the loading reached 40,000 times. Interestingly, increasing asphalt thickness every 5 cm will increase the vertical compressive stress in the asphaltic underlayment tracks in a uniform percentage, 1%.

Table 7 displays the regression formula based on the numerical modeling outputs used to predict the vertical compressive stress magnitudes at the subgrade surface in the conventional and the asphaltic underlayment tracks as the loading reached 500,000 times. It was estimated that the vertical compressive stress in Case 1A, Case 1B, and Case 1C (conventional track) after 500,000 loading cycles was 10.0484 MPa, 10.2089 MPa, and 10.5875 MPa. Meanwhile, the vertical compressive stress in Case 2A, Case 2B, and Case 2C (asphaltic underlayment tracks) obtained 9.3915 MPa, 9.4665 MPa, and 9.5380 MPa, respectively.

As described in Fig. 7 and Table 7, the asphaltic underlayment tracks had a more uniform structural performance and produced lower vertical compressive stress at the surface of the subgrade layer. Although the asphaltic underlayment tracks had a structural thickness of 20 cm thinner than the conventional tracks, their performance was superior in reducing and transmitting the stress from the loading cycles of the Babaranjang trains.

Setiawan [52] investigated and compared the response of all-granular tracks with various ballast and sub-ballast thicknesses (10.5 inches, 14 inches, and 21 inches) and asphaltic overlayment tracks with various asphalt layer thicknesses (7.87 inches, 10.63 inches, and 13.78 inches) subjected to different load repetitions (500,000; 1,000,000; and 2,000,000) using the mechanistic-empirical approach. It was discovered that the asphaltic overlayment tracks better transmitted the top stresses, therefore reducing subgrade compressive stresses.

Setiawan [53] predicted the subgrade service life of ballasted, asphaltic underlayment, and combination tracks by varying the sub-ballast layer (0, 5, 10, 15, 20, 25, and 30 cm) and the asphalt layer thickness (0, 5, 10, 15, 20, 25, and 30 cm) according to the magnitude of compressive stress at the surface of the subgrade using the KENTRACK program. In summary, the asphaltic underlayment tracks had the longest subgrade service life, followed by the combination tracks and the all-granular tracks due to the lower compressive stress at the surface of the subgrade layer.

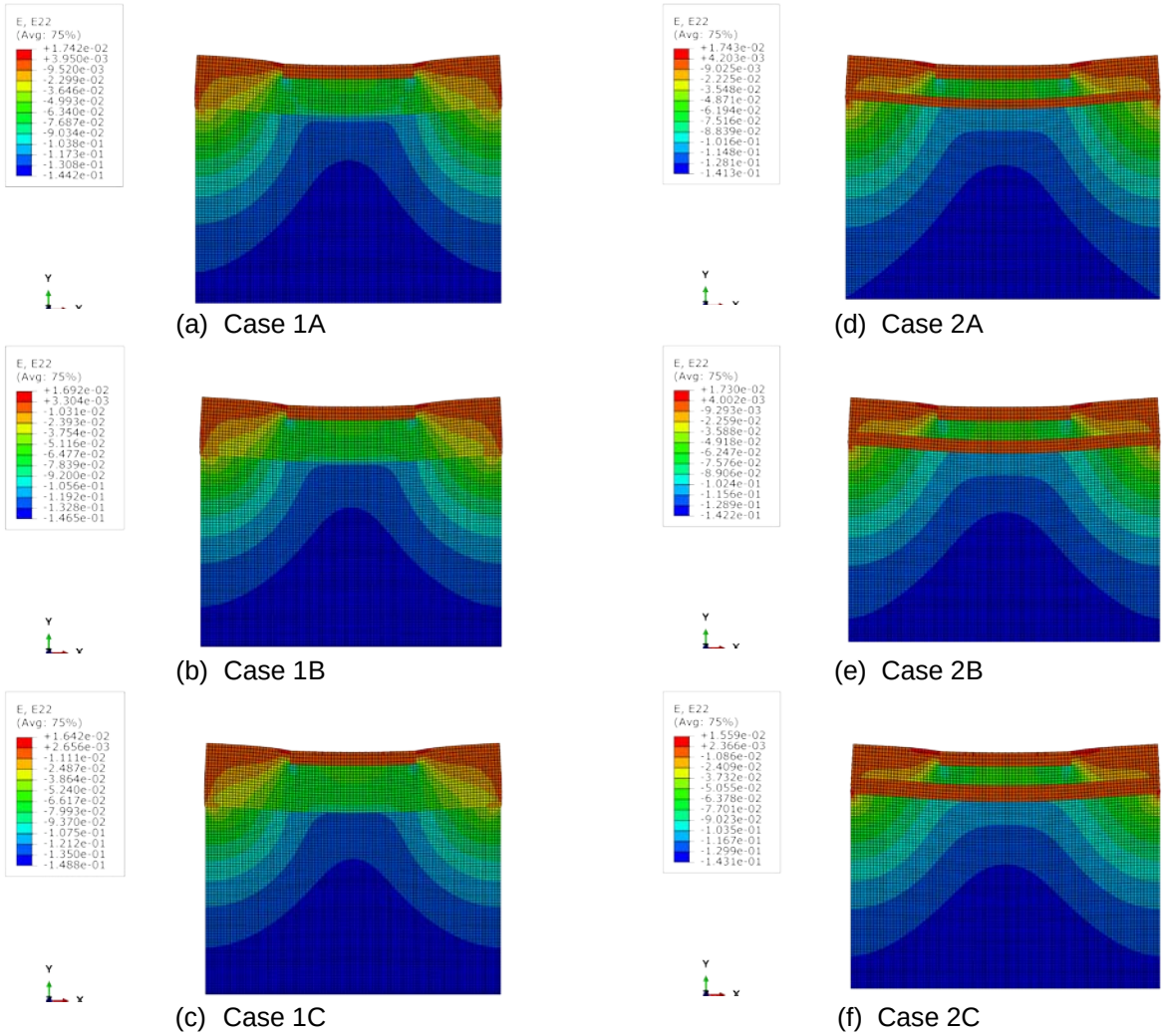

Fig. 9. Vertical strain distribution in the conventional tracks (a, b, c) and the asphaltic underlayment tracks (d, e, f)

3.2 Measurement of strain component

Fig. 8 demonstrates the numerical simulation results of horizontal strain distribution in the conventional and the asphaltic underlayment tracks as the loading reached 40,000 times. The horizontal strain distribution in the asphaltic underlayment tracks was more uniform and well-distributed than in the conventional ones, especially in the area below the sleeper. Also, there was almost no difference in the horizontal strain distribution between Case 2A (15 cm of asphalt), Case 2B (20 cm of asphalt), and Case 2C (25 cm of asphalt). On another side, there was a quite significant difference in the horizontal strain distribution between Case 1A (30 cm of sub-ballast), Case 1B (40 cm of sub-ballast), and Case 1C (50 cm of sub-ballast).

The numerical simulation results of vertical strain distribution in the conventional and the asphaltic underlayment tracks as the loading reached 40,000 times are depicted in Fig. 9. It can be observed that both track types experienced more vertical compressive (-) strain than vertical tensile (+) strain. In the conventional tracks, only the sleeper and top part of the ballast experienced the vertical tensile (+) strain. In the asphaltic underlayment tracks, both the sleeper and asphalt layer and the top part of ballast experienced the vertical tensile (+) strain.

The numerical simulation results of maximum strain in-plane principal distribution in the conventional and the asphaltic underlayment tracks after 40,000 loading cycles are presented in Fig. 10. In the conventional tracks, the maximum tensile (+) strain in-plane principal became lower, but its area became wider as the sub-ballast thickness became thicker. On another side, the maximum compressive (-) strain in-plane principal became higher, but its area got narrower as the sub-ballast thickness became thicker (please see Fig. 10a, Fig. 10b, and Fig. 10c). Also, it is obvious that the highest tensile (+) occurred and was concentrated at the interface between the sleeper's side

and the ballast layer. It would grow to create a parabolic shape as the sub-ballast layer became thicker. Furthermore, the highest compressive (-) was concentrated from the edge-surface of the subgrade layer, where the boundary conditions were determined for the 2-dimension modeling developed in this study.

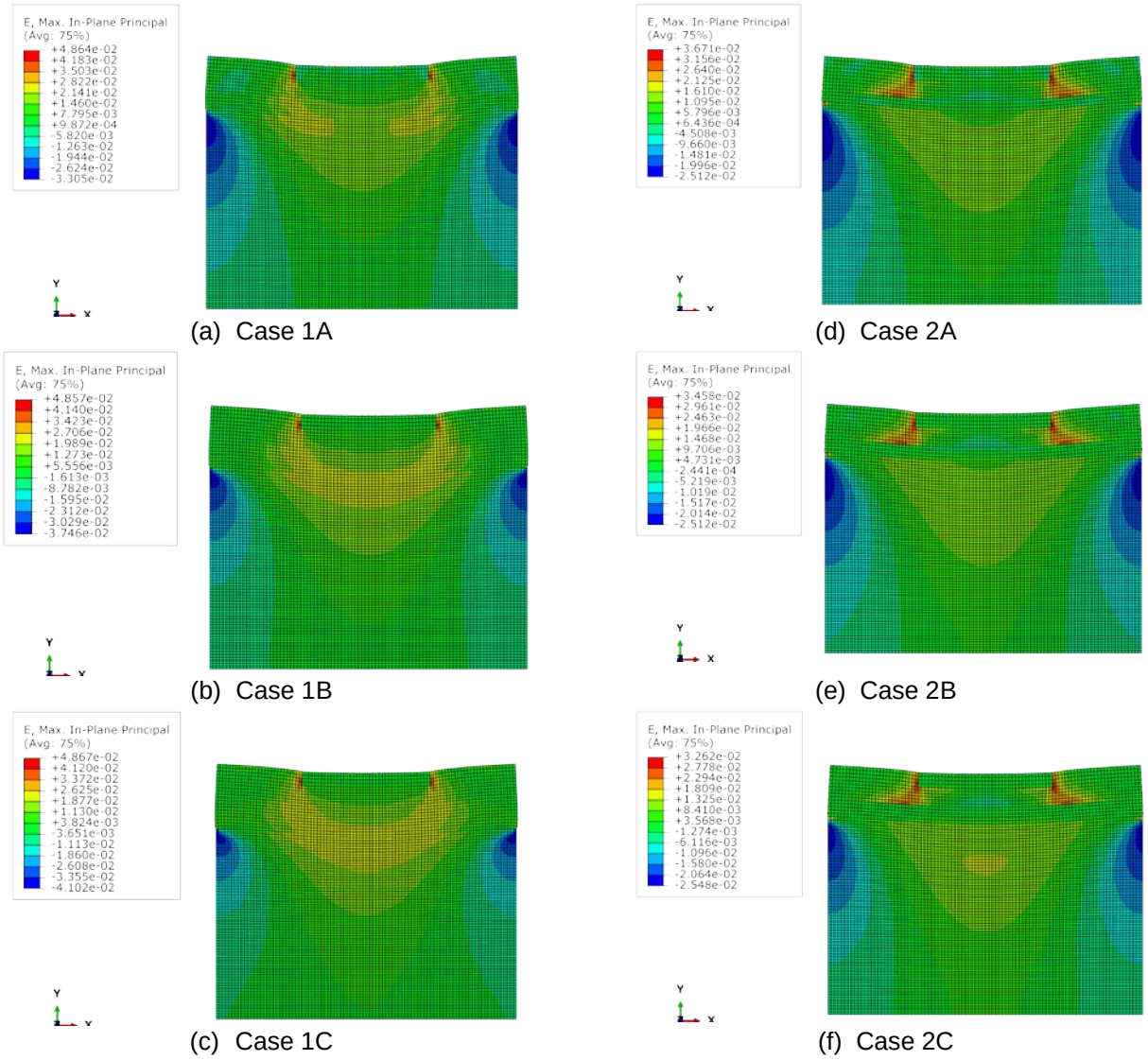

Fig. 10. Maximum strain in-plane principal distribution in the conventional tracks (a, b, c) and asphaltic underlayment tracks (d, e, f)

In the asphaltic underlayment tracks, the maximum tensile (+) strain in-plane principal became higher, and its area became wider as the asphalt thickness became thicker. On the other hand, the maximum compressive (-) strain in-plane principal became lower, and its area turned narrower as the asphalt thickness got thicker (please see Fig. 10d, Fig. 10e, and Fig. 10f). In addition, the highest tensile (+) was concentrated near the interface area of the sleeper's side and the ballast layer, developed until it reached the bottom part of the ballast layer. Furthermore, the highest compressive (-) was also concentrated from the edge-surface of the subgrade layer, where the boundary conditions were determined for the 2-dimension modeling developed in this study.

Therefore, in general, the magnitude of both the maximum tensile and maximum compressive strain in-plane principal in the asphaltic underlayment tracks was lower than in the conventional tracks, and the distribution area of both the maximum tensile and maximum compressive strain in-plane principal in the asphaltic underlayment tracks was more uniform and well-distributed than in the conventional tracks.

3.3 Measurement of deformation

In this study, the deformation presented in Fig. 11 was based on the relative displacement between the surface of the sleeper and the surface of the subgrade. Fig. 11 exhibits the numerical simulation results of the ballast and the sub-ballast layers' deformation in the conventional tracks (Fig. 11a, Fig. 11b, and Fig. 11c) and the ballast and the asphalt layers' deformation in the asphaltic underlayment tracks (Fig. 11d, Fig. 11e, and Fig. 11f).

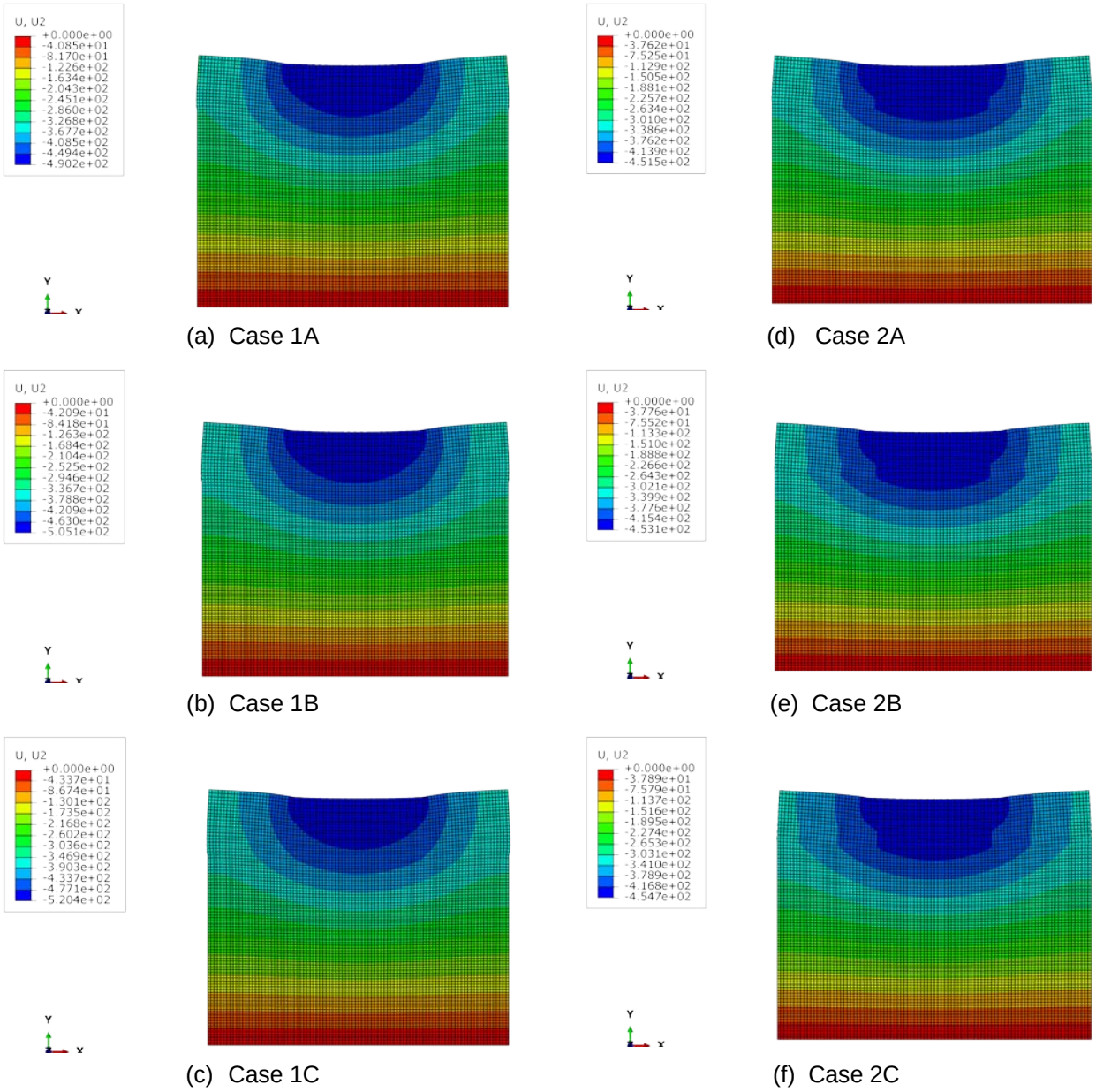

Fig. 11. Numerical simulation results of ballast and sub-ballast layers' deformation in the conventional tracks (a, b, c) and ballast and asphaltic layers' deformation in the asphaltic underlayment tracks (d, e, f)

The displacement bulb was continuously developed through the ballast and sub-ballast layers in the conventional tracks. It was because both ballast and sub-ballast had similar mechanical properties in terms of elastic modulus (130 MPa vs. 120 MPa), Poisson's ratio (0.20 vs. 0.30), and mass density (1,900 kg/m3 vs. 1900 kg/m3). On the other hand, a discontinuity can be seen in the displacement bulb inside the ballast and asphalt layers in the asphaltic underlayment tracks. It became more significant as the asphalt layer got thicker. It was because both ballast and asphalt used in this study had significantly different mechanical properties in terms of elastic modulus (130 MPa vs. 4000 MPa), Poisson's ratio (0.20 vs. 0.35) and mass density (1,900 kg/m3 vs. 2400 kg/m3).

Fig 12 illustrates the displacement at the top of the sleeper and the subgrade layer in the conventional tracks (Fig. 12a, Fig. 12b, and Fig. 12c) and the asphaltic underlayment tracks (Fig. 12d, Fig. 12e, and Fig. 12f). It can be inferred that the thicker the sub-ballast layer in the conventional tracks, the higher the displacement at the top of the sleeper and the subgrade layer. In addition, the thicker the sub-ballast in the conventional tracks, the higher the displacement differences between the top of the sleeper and the surface of the subgrade layer. With the sub-ballast layer thickness of 30 cm (Case 1A), 40 cm (Case 1B), and 50 cm (Case 1C), the measurement results depicted the displacement at the top of the sleeper and the top of the subgrade of 385.76 mm and 356.39 mm for Case 1A (Fig. 12a), 399.63 mm and 364.44 mm for Case 1B (Fig. 12b), and 413.93 mm and 372.63 mm for Case 1C (Fig. 12c), respectively, as the loading reached 40,000 times.

The asphaltic underlayment tracks have demonstrated different trends. The displacement magnitude at the top of the sleeper and the top of the subgrade layer in Case 2A (Fig. 12d), Case 2B (Fig. 12e), and Case 2C (Fig. 12f)

was almost similar. With the asphalt layer thickness of 15 cm (Case 2A), 20 cm (Case 2B), and 25 cm (Case 2C), the measurement attained the displacement at the top of the sleeper and the top of the subgrade of 355.07 mm and 341.54 mm for Case 2A (Fig. 12d), 358.12 mm and 344.46 mm for Case 2B (Fig. 12e), and 361.12 mm and 347.16 mm for Case 2C (Fig. 12f), respectively, as the loading reached 40,000 times.

(a) Case 1A

(d) Case 2A

(b) Case 1B

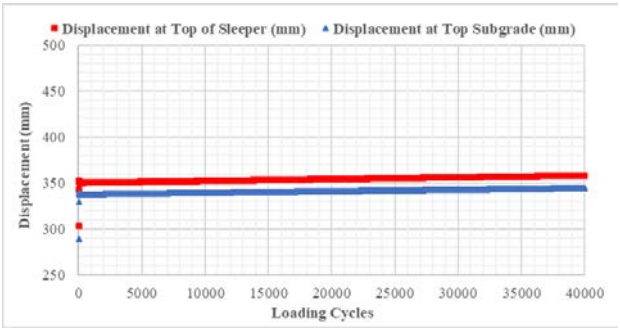

(e) Case 2B

(c) Case 1C

(f) Case 2C

Fig. 12. Displacement at the surface of the sleeper and the surface of the subgrade layer in the conventional tracks (a, b, c) and the asphaltic underlayment tracks (d, e, f)

Fig. 13 illustrates the growth of the ballast and sub-ballast deformation in the conventional tracks and the growth of the ballast and asphalt deformation in the asphaltic underlayment tracks and their magnitude as the loading reached 40,000 times. Table 8 presents the regression formula based on the numerical simulation results used to predict the ballast and sub-ballast deformation in the conventional tracks and the ballast and asphalt deformation in the asphaltic underlayment tracks after 500,000 loading cycles. As displayed in Fig 13, the deformation in the asphaltic underlayment tracks is almost three times lower than that in the conventional tracks. Based on the numerical modeling outputs in Table 8, the increase of sub-ballast thickness every 10 cm will increase the deformation in the conventional tracks up to 20% (29.38 mm in Case 1A vs. 35.19 mm in Case 1B vs. 41.30 mm in Case 1C). However, the increase of asphalt thickness every 5 cm will increase the deformation in the asphaltic underlayment tracks only between 1% (from 13.52 mm in Case 2A to 13.66 mm in Case 2B) and 2% (from 13.66 mm in Case 2B to 13.96 mm in Case 2C). In conclusion, the deformation magnitude of the asphaltic underlayment tracks in Case 2A, Case 2B, and Case 2C was almost similar.

A Babaranjang train set consists of 50 coal cars. Forty thousand loading cycles in this study equal 20,000 coal carriages or the same with 400 Babaranjang train sets. Therefore, 500,000 loading cycles equal 250,000 coal carriages or the same with 5,000 Babaranjang train sets. Around ten Babaranjang trains are operated per day. Therefore, it was predicted that after serving 5,000 Babaranjang train sets, the conventional tracks in Case 1A, Case 1B, Case 1C would experience 47.72 mm, 58.29 mm, and 64.16 mm of deformation, respectively (please see Table 8 column 5). Meanwhile, the estimated deformation in the asphaltic underlayment tracks after serving 5,000

Babaranjang train sets are 22.62 mm (Case 2A), 22.75 mm (Case 2B), and 23.02 mm (Case 2C), respectively (please see Table 8 column 5).

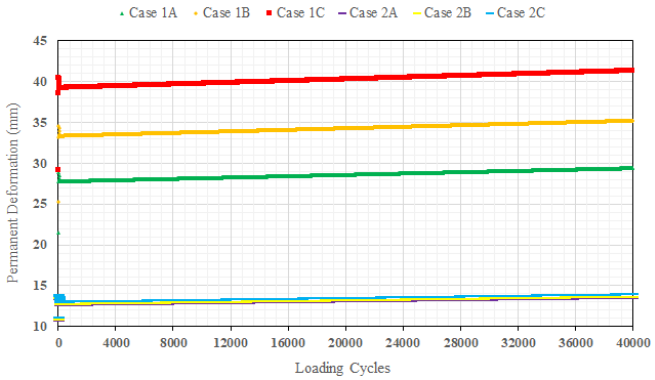

Fig. 13. Growth of the ballast and sub-ballast deformation in the conventional tracks and the growth of the ballast and asphalt deformation in the asphaltic underlayment tracks

Table 8. Deformation (mm) after 40,000 loading cycles and regression formula to predict deformation after 500,000 loading cycles

Track type	Case	Deformation (mm) after 40,000 Loading Cycles	Regression Formula	Predicted Deformation (mm) after 500,000 Loading Cycles
Conventional	1A	29.38	y = 4E-05x + 27.72	47.72
	1B	35.19	y = 5E-05x + 33.29	58.29
	1C	41.30	y = 5E-05x + 39.16	64.16
Asphaltic Underlayment	2A	13.52	y = 2E-05x + 12.62	22.62
	2B	13.66	y = 2E-05x + 12.75	22.75
	2C	13.96	y = 2E-05x + 13.02	23.02

By comparing Fig. 13 and Fig. 7,it can be inferred that the asphaltic underlayment tracks have a more uniform structural performance and lower deformation than the conventional tracks because the asphalt layer in the asphaltic underlayment is significantly stiffer than the sub-ballast layer in the conventional tracks. The thicker the sub-ballast and asphalt layer, the higher the possibility of deformation due to loading. Lee et al. [47] discovered that the thicker asphalt layer in the asphaltic overlayment tracks deforms slightly more than the thinner layer.

4 CONCLUSIONS

The behaviors of different structures of the conventional and asphaltic underlayment tracks under cyclic loading conditions of Babaranjang (long-chain coal) freight trains have been evaluated in this study using numerical simulation and by considering linear elastic behavior of all materials in both rail track types, characterized by the elastic modulus, Poisson's Ratio, and mass density. This research investigated and analyzed the vertical compressive stress, horizontal-vertical strain, and deformation behavior. According to the numerical simulation, the measurement of vertical compressive stress indicates that the asphaltic underlayment track structure was superior in reducing and transmitting the stress generated by train loading. In addition, the measurement of horizontal-vertical-maximum strain implies that the asphaltic underlayment tracks had a more uniform structural strength than the conventional tracks. Based on deformation measurement, asphaltic underlayment tracks had a more uniform structural performance and lower deformation than the conventional tracks. Moreover, increasing the thickness of the ballast and sub-ballast layers (more than the standard thickness, 30 cm) as the effort in reconstructing Indonesia's conventional tracks after the train derailment could worsen its condition, resulting in higher deformation magnitude. Furthermore, the deformation magnitude of asphaltic underlayment tracks with 15 cm, 20 cm, and 25 cm was almost similar. Therefore, asphalt thickness of 15 cm below the ballast layer seems appropriate to support the freight trainload. For future research, it is worth applying numerical simulation considering the linear viscoelastic behavior of asphalt layer in asphaltic underlayment tracks subjected to the heavy-low speed freight train loading in existing Indonesia's railway systems and to the high-speed train loading in future Indonesia's railway systems.

5 REFERENCES

[1] MP3EI Masterplan. (2011). Acceleration and expansion of Indonesia economic development and national connectivity enhancement, Published by Co-ordinating Ministry of Economic Affairs, Jakarta.

[2] Woroniuk, C., Aditjandra, P., Zunder, T. H. (2014). An investigation into rail freight capacity in Indonesia. Transport Research Arena, Paris.

[3] Bahagia, S., Sandee, H., Meeuws, R. (2013). State of logistics Indonesia 2013, Collaboration Center of Logistics and supply chain studies, InstitutTeknologi Bandung, AsosiasiLogistik Indonesia, Panteia, STC Group and World Bank.

[4] BadanPusatStatistik. Panjangjaringanjalanrelkeretaapi di Indonesia (km), 2015-2017 (Title in English: Length of railroad network in Indonesia (km), 2015-2017), from https://www.bps.go.id/indicator/17/1195/1/panjang-jaringan-jalan-rel-kereta-api-di-indonesia-.html, accessed on 2021-12-19.

[5] Sekretariat Negara. (2012). Minister of transportation regulation no. 60 of 2012 concerning railroad technical requirements (Title in English: Peraturanmenteriperhubungan no. 60 tahun 2012 tentangpersyaratanteknisjalurkeretaapi). Jakarta.

[6] Dikun, S. (2010). Future Indonesian railways: An interface report towards the national railway master plan, Indonesia Infrastructure Initiative.

[7] Kompas. Viral, video keretaapibabaranjangalamianjlokhinggagerbongterguling (Title in English: Viral, video of the babaranjang train derailed until the carriage overthrows), from https://www.kompas.com/tren/read/2021/12/11/205000065/viral-video-kereta-api-babaranjang-alami-anjlok-lokomotif-hingga-gerbong, accessed on 2021-12-19.

[8] Merdeka. 6 Gerbongkeretaangkutbatubaraanjlok di MuaraEnim (Title in English: 6 Carriage of coal hauling train derails in MuaraEnim), from https://www.merdeka.com/peristiwa/6-gerbong-kereta-angkut-batubara-anjlok-di-muara-enim.html, accessed on 2021-12-19.

[9] Setiawan, D. M., Rosyidi, S. A. P. (2017). Track quality index as track quality assessment indicator. Proceeding of the 19th International Symposium of Indonesian Inter-University Transportation Studies Forum (FSTPT), Universitas Islam Indonesia, Indonesia, Ch. 2, p. 197-207.

[10] Alves Costa, P., Calcada, R., Cardoso, A.S., Bodare, A. (2010). Influence of soil non-linearity on the dynamic response of high-speed railway tracks. Soil Dynamics and Earthquake Engineering, vol. 30, 221-235, DOI: http://dx.doi.org/10.1016/j.soildyn.2009.11.002

[11] Sol-Sanchez, M., Pirozzolo, L., Moreno-Navarro, F., Rubio-Gamez, M. C. (2015). Advanced characterisation of bituminous sub-ballast for its application in railway tracks: The influence of temperature. Construction and Building Materials, vol. 101, 338-346, DOI: https://doi.org/10.1016/j.conbuildmat.2015.10.102

[12] Sol-Sanchez, M., Pirozzolo, L., Moreno-Navarro, F., Rubio-Gamez, M. C. (2016). A study into the mechanical performance of different configurations for the railway track section: A laboratory approach. Engineering Structures, vol. 119, 12-23, DOI: http://dx.doi.org/10.1016/j.engstruct.2016.04.008

[13] Signes, C. H., Fernandez, P. M., Garzon-Roca, J., de la Torre, M. E. G., Franco, R. I. (2016). An evaluation of the resilient modulus and deformation of unbound mixtures of granular materials and rubber particles from scrap tyres to be used in subballast layers. Transportation Research Procedia, vol. 18, 384-391, DOI: https://doi.org/10.1016/j.trpro.2016.12.050

[14] du Plooy, R., Grabe, H. (2017). Characterisation of rigid polyurethane foam‐reinforced ballast through cyclic loading box tests. Journal of the South African Institution of Civil Engineering, vol. 59, no. 2, 2-10, DOI: http://dx.doi.org/10.17159/2309-8775/2017/v59n2a1

[15] Sol-Sanchez, M., D'Angelo, G. (2017). Review of the design and maintenance technologies used to decelerate the deterioration of ballasted railway tracks. Construction and Building Materials, vol. 157, 402-415, DOI: https://doi.org/10.1016/j.conbuildmat.2017.09.007

[16] Setiawan, D. M., Rosyidi, S. A. P. (2018). Vertical deformation and ballast abrasion characteristics of asphalt-scrap rubber track bed. International Journal on Advanced Science, Engineering and Information Technology, vol. 8, no. 6, 2479-2484, DOI: https://doi.org/10.18517/ijaseit.8.6.7411

[17] Setiawan, D. M., Rosyidi, S. A. P., Budiyantoro, C. (2019). The role of scrap rubber, asphalt, and manual compaction against the quality of ballast layer. Jordan Journal of Civil Engineering, vol. 13, no. 4, 594-608.

[18] Rosyidi, S. A. P., Setiawan, D. M., Budiyantoro, C., Bintari, L.N. (2019). The role of scrap rubber size against the characteristics of ballast layer. IOP Conf. Series: Materials Science and Engineering, 650, 1-10, DOI: https://doi.org/10.1088/1757-899X/650/1/012052

[19] Setiawan, D. M. (2019). Utilization of 60/70 penetration grade asphalt on ballast structures with the variation of percentage and the number of pouring layers. Journal of the Mechanical Behavior of Materials, vol. 28, no. 1, 107-118, DOI: https://doi.org/10.1515/jmbm-2019-0013

[20] Setiawan, D. M., Rosyidi, S. A. P. (2019). Scrap rubber and asphalt for ballast layer improvement. International Journal of Integrated Engineering, vol. 11, no. 8, 247-258, DOI: https://doi.org/10.30880/ijie.2019.11.08.025

[21] Kollo, S. A., Puskas, A., Kollo, G. (2020). Rubber as a vital component of railway tracks. Procedia Manufacturing, vol. 46, 202-208, DOI: https://doi.org/10.1016/j.promfg.2020.03.030

[22] Zbiciak, A., Kraśkiewicz, C., Sabouni-Zawadzka, A. A. Pełczyński J, Dudziak S. (2020). A novel approach to the analysis of under sleeper pads (usp) applied in the ballasted track structures. Materials, vol. 13, 2438, DOI: https://doi.org/10.3390/ma13112438

[23] Barbieri, D. M., Tangeras, M., Kassa, E., Hoff, I., Liu, Z., Wang, F. (2020). Railway ballast stabilising agents: Comparison of mechanical properties. Construction and Building Materials, vol. 252, 119041, DOI: https://doi.org/10.1016/j.conbuildmat.2020.119041

[24] Setiawan, D. M. (2021). Application of 60/70 grade bitumen with layer variations on ballast structures. International Journal on Advanced Science, Engineering and Information Technology, vol. 11, no. 2, 698-704, DOI: https://doi.org/10.18517/ijaseit.11.2.9898

[25] Wang, J., Zeng, X. (2004). Numerical simulations of vibration attenuation of high-speed train foundations with varied trackbed underlayment materials. Journal of Vibration and Control, vol. 10, 1123-1136, DOI: https://doi.org/10.1177/1077546304043268

[26] Zeng, X. (2005). Rubber-modified asphalt concrete for high-speed railway road. Final Report for High-Speed Rail IDEA Project 40. Case Western Reserve University Cleveland, Ohio, United States.

[27] Teixeira, P. F., López-Pita, A., Casas, C. (2006). Improvements in high-speed ballasted track design: benefits of bituminous sub-ballast layers. Transportation Research Record: Journal of the Transportation Research Board, 1943, 43-49.

[28] Lei, X., Rose, J. G. (2008). Numerical investigation of vibration reduction of ballast track with asphalt trackbed over soft subgrade. Journal of Vibration and Control, vol. 14. no. 12, 1885-1902, DOI: https://doi.org/10.1177/1077546308091213

[29] Liu, X., Zhao, P., Dai, F. (2011). Advances in design theories of high-speed railway ballastless tracks. Journal of Modern Transportation, vol. 19, no. 3, 154-162, DOI: http://dx.doi.org/10.1007/BF03325753

[30] Fang, M., Qiu, Y., Rose, J., West. R., Ai, C. (2011). Comparative analysis on dynamic behavior of two HMA railway substructures. Journal of Modern Transportation, vol. 19, no. 1, 26-34, DOI: https://doi.org/10.3969/j.issn.2095-087X.2011.01.005

[31] Lei, X., Zhang, B. (2011). Analysis of dynamic behavior for slab track of high-speed railway based on vehicle and track elements. Journal of Transportation Engineering, vol. 137, no. 4, 227-240, DOI: https://doi.org/10.1061/(ASCE)TE.1943-5436.0000207

[32] Fang, M., Cerdas, S. F., Qiu, Y. (2013). Numerical determination for optimal location of sub-track asphalt layer in high-speed rails. Journal of Modern Transportation, vol. 21, no. 2, 103-110, DOI: https://doi.org/10.1007/s40534-013-0012-0

[33] Chen, R., Zhao, X., Wang, Z., Jiang, H., Bian, X. (2013). Experimental study on dynamic load magnification factor for ballastless track-subgrade of high-speed railway. Journal of Rock Mechanics and Geotechnical Engineering, vol. 5, 306-311, DOI: http://dx.doi.org/10.1016/j.jrmge.2013.04.004

[34] Chen, R. P., Chen, J. M., Wang, H. L. (2014). Recent research on the track-subgrade of high-speed railways. Journal of Zhejiang University-SCIENCE A (Applied Physics & Engineering), vol. 15, no. 12, 1034-1038, DOI: https://doi.org/10.1631/jzus.A1400342

[35] Wang, P., Xu, H., Chen, R. (2014). Effect of cement asphalt mortar debonding on dynamic properties of CRTS II slab ballastless track. Advances in Materials Science and Engineering, 193128, 1-8, DOI: https://doi.org/10.1155/2014/193128

[36] Ramirez Cardona, D., Benkahla, J., Costa, D., Calon, N., Robinet, A., Di Benedetto, H., Sauzeat, C. (2014). High-speed ballasted track behavior with sub-ballast bituminous layer. Conference: GeoRail, Marne-laVallee, France.

[37] Fang, M., Cerdas, S. F. (2015). Theoretical analysis on ground vibration attenuation using sub-track asphalt layer in high-speed rails. Journal of Modern Transportation, vol. 23, no. 3, 214-219, DOI: https://doi.org/10.1007/s40534-015-0081-3

[38] Lee, S. H., Choi, Y. T., Lee, H. M., Park, D. W. (2016). Performance evaluation of directly fastened asphalt track using a full-scale test. Construction and Building Materials, vol. 113, 404-414, DOI: http://dx.doi.org/10.1016/j.conbuildmat.2016.02.221

[39] Bouraima, M. B., Yang, E., Qiu, Y. (2017). Mechanics calculation of asphalt concrete track-substructure layer and comparisons. American Journal of Engineering Research (AJER), vol. 6, no. 7, 280-287.

[40] Liu, Y., Qian, Z. D., Zheng, D., Huang, Q. B. (2018). Evaluation of epoxy asphalt-based concrete substructure for high-speed railway ballastless track. Construction and Building Materials, vol. 162, 229-238, DOI: https://doi.org/10.1016/j.conbuildmat.2017.12.028

[41] Zhu, S., Wang, M., Zhai, W., Cai, C., Zhao, C., Zeng, D. (2018). Mechanical property and damage evolution of concrete interface of ballastless track in high-speed railway: Experiment and simulation. Construction and Building Materials, vol. 187, 460-473, DOI: https://doi.org/10.1016/j.conbuildmat.2018.07.163

[42] Setiawan, D. M., Muthohar, I., Ghataora, G. (2013). Conventional and unconventional railway for railways on soft ground in Indonesia (Case study: rantauprapat-duri railways development). Proceeding of the 16th FSTPT International Symposium, UniversitasMuhammadiyah Surakarta, p. 610-620.

[43] Huang, Y. H., Lin, C., Deng, X. (1984). Hot mix asphalt for railroad trackbeds – Structural analysis and design. Technical sessions, Association of asphalt pavingtechnologists, Scottsdale, Arizona, p. 475-494.

[44] Rose, J. G., Bryson, L. S. (2009). Optimally designed hot mix asphalt railway trackbeds–Test measurements, trackbed materials, performance evaluations and significant implications. The International Conference on Perpetual Pavements, Ohio Research Institute for Transportation and Environment, Columbus Ohio, United States.

[45] Robinet, A., Cuccaroni, A. (2012). L'expérience grave-bitume de la LGV Est Européenne [Title in English: The bituminous mixture experience of the East European HSL], Revue générale des chemins de fer (RGCF) 220, p. 44-50.

[46] Ramirez Cardona, D., Di Benedetto, H., Sauzeat, C., Calon, N., Saussine, G. (2016). Use of a bituminous mixture layer in high-speed line trackbeds. Construction and Building Materials, vol. 125, 398-407, DOI: https://doi.org/10.1016/j.conbuildmat.2016.07.118

[47] Lee, S. H., Vo, H. V., Park, D. W. (2018). Investigation of asphalt track behavior under cyclic loading: full-scale testing and numerical simulation. Journal of Testing and Evaluation, vol. 46, no. 3, 934-942, DOI: https://doi.org/10.1520/JTE20160554

[48] Hassan, A. G., Khalil, A. A., Ramadan, I., Metwally, K. G. (2020). Investigation of using a bituminous sub-ballast layer to enhance the structural behavior of high-speed ballasted tracks. International Journal of GEOMATE, vol. 19, no. 75, 22-132, DOI: https://doi.org/10.21660/2020.75.27822

[49] Rosyidi, S. A. P. (2015). Rekayasa jalan kereta api: tinjauan struktur jalan rel. Yogyakarta: Lembaga Penelitian, Publikasi dan Pengabdian Masyarakat Universitas Muhammadiyah Yogyakarta (LP3M-UMY), Yogyakarta, Indonesia.

[50] Wang, X., Pu, J., Wu, P., Chen, M. (2020). Modeling of coupling mechanism between ballast bed and track structure of high-speed railway. Mathematical Problems in Engineering, 9768904, DOI: https://doi.org/10.1155/2020/9768904

[51] Liu, S. (2013). KENTRACK 4.0: A railway track-bed structural design program. Theses and Dissertations. Department of Civil Engineering. University of Kentucky, USA.

[52] Setiawan, D. M. (2021). Structural response and sensitivity analysis of granular and asphaltic overlayment track considering linear viscoelastic behavior of asphalt. Journal of the Mechanical Behavior of Materials, vol. 30, no. 1, 66-86, DOI: https://doi.org/10.1515/jmbm-2021-0008

[53] Setiawan, D. M. (2022). Sub-grade service life and construction cost of ballasted, asphaltic underlayment, and combination rail track design. Jordan Journal of Civil Engineering, vol. 16, no. 1, 173-192.

Paper submitted: 21.12.2021.

Paper accepted: 16.02.2022.